Online Optimal Switching of Single Phase DC/AC Inverters using Partial Information

Kyriakos G. Vamvoudakis, João P. Hespanha

***Abstract*— This paper proposes an online optimal tracking algorithm to provide the desired voltage magnitude and frequency at the load. This eventually will work as a DC/AC microinverter that with appropriate switching of semiconductor devices will convert low DC voltage to high AC voltage. An $L-C$ filter is used to reduce the effects caused by switching semiconductor devices. The proposed control scheme ensures a good tracking of an exosystem that provides the desired voltage magnitude and frequency. It builds upon the ideas of approximate dynamic programming (ADP) and uses only partial information of the system and exosystem. A Lyapunov stability proof ensures that the closed-loop system is asympotically stable. Finally, simulations show the effectiveness of the proposed approach.**

***Index Terms*— Power systems, voltage source inverter, approximate dynamic programming.**

I. Introduction

Optimal control offers a significant framework for savings by optimizing the functional behavior of any power system. Independent electric energy systems are untethered from the electrical utility grid. Their common bond is energy storage (i.e. batteries), which absorbs and releases energy in the form of direct current (DC) electricity. Increasing use of renewable energy sources [5] with intermittent generation requires more flexible ("smarter") ways of balancing power consumption and generation. In contrast, the utility grid supplies with alternating current (AC) electricity. AC is used for grid service because it is more practical for long distance transmission.

There are ways to use DC directly, but for a modern lifestyle, one needs a voltage source inverter (VSI) for the vast majority of the appliances. VSIs are involved in a wide range of applications including electric motor drivers, electric/hybrid cars power supply, naval ships, or industrial power systems [2]. Today the inverters have lower losses, better power quality, are cheaper and more available for high power applications. The same converters can operate with reverse power flow and transfer power from the system alternating voltage DC system voltage. In this case they are called rectifiers [9]. Thus, the inverter DC/AC can be used in a multitude of applications and successfully replace the operation of other electronic devices power as the rectifier diodes or thyristors. The control of VSI has become an important research topic, and many control methods have been proposed to optimize its performance. Control schemes that are usually designed for power system models are simplified and even if good power system models exist, they never represent truly the real power system. To overcome this problem, one needs to design robust algorithms that adapt themselves to the changing environment by adjusting their performance and allowing plant uncertainties. Reinforcement learning methods allow learning of new controllers based on the interactions with the environment [15].

K. G. Vamvoudakis, J. P. Hespanha are with the Center for Control, Dynamical-systems and Computation (CCDC), University of California, Santa Barbara, CA 93106-9560 USA e-mail: kyriakos@ece.ucsb.edu, hespanha@ece.ucsb.edu.

*This material is based upon work supported in part by ARO MURI Grant number W911NF0910553 and ARO grant W911NF-09-D-0001 (Inst. for Collaborative Biotechnologies).

Related work

Control systems for power systems [14] and specifically for voltage inverters usually use PI control [21], deadbeat control [11], or a combination of them [4], [20] delta modulation, hysteresis control [26], or even more complex multivariable feedback control [8], [16], [17], [27]. Most of the aforementioned control algorithms are performed in the phasor domain and use modulation techniques without optimality guarantees. A basic designer dilemma is the compromise between the number of measurements and the complexity of the circuit that the control system uses. Control systems that measure less variables are being implemented with increased complexity. The variables that cannot be measured in the circuit, need to be identified with observers [3], [4]. The observers enter a delay in the system because of the increased calculations and complexity. In practice it is impossible to know exactly all the parameters of the filter connected to the inverter since most of them change with time. It is necessary that the control system allows uncertainties without losing its optimal performance.

Recently, computational intelligence methods have been used widely in optimizing excitation controllers and maintaining the appropriate terminal voltage, increase real-time responsiveness to changing power loads, component failures, improvement of transient behavior of power systems by using optimal neuro-adaptive control ideas [7], [18], [22]. A recent survey stating the need for computational intelligent controllers that allows the smart grid to self-heal, resist attacks, allow dynamic optimization of the operation, improve power quality and efficiency is presented in [24]. The authors in [12] present and apply a robust ADP framework to handle parameter uncertainties in a two-machine power system. The chapter in [23] presents application examples through simulations and experiments in the field of power systems control using adaptive-critic designs but most of them require full knowledge of the power system dynamics and are designed for discrete-time systems.

Preprint submitted to 2014 American Control Conference.
Received September 27, 2013.

Contributions

The contributions of the present paper are threefold. First, this paper proposes a new ADP algorithm with the ability to produce high AC voltage from low DC voltage by optimizing a prescribed performance. Also, the proposed framework does not require any plant parameter estimation, but instead, plant information is used to find the controller parameters directly online. An exosystem is used to produce a potentially unknown frequency and amplitude to the load. The algorithm implemented only requires measurements of the current, the voltage and the value of the inductance L, in the $L-C$ filter connected to the voltage source inverter. By using an appropriate value for the user defined matrix in the performance we can achieve asymptotic tracking of the exosystem with guaranteed optimality.

Organization

The paper is structured as follows. Section II formulates the problem of converting low DC voltage to high AC voltage with guaranteed performance. In Sections III, we present an integral reinforcement learning algorithm to solve the optimal control voltage source inverter problem online with partial information. Simulation results showing the efficacy of the approach are presented in Section IV. Finally Section V concludes and talks about future work.

Notation: For the ease of readers, we provide here a partial notation list. Thus, $\mathbb{R}^+$ denotes the set $\{x \in \mathbb{R} : x > 0\}$. Moreover we write $\underline{\lambda}(M)$ for the minimum eigenvalue of matrix M and $\bar{\lambda}(M)$ for the maximum.

II. Problem Formulation

The goal is to design an intelligent control algorithm to convert low DC voltage to high AC voltage by appropriately opening and closing switches to achieve $\pm V_{\rm dc}$, namely a single phase inverter, with guaranteed optimal performance and with the least knowledge of the system.

In order to achieve the desired frequency and magnitude at the load (in the form of $V_C = \sqrt{2}V cos(\omega_0 t + \zeta)$ where V is the rms value of the phase voltage, $\omega_0 \in \mathbb{R}^+$ is the frequency and ζ is the phase angle) we will use the following antistable ($Re\{\sigma(Z) = 0\}$) exosystem initialized at the right amplitude as,

$$\dot{Z} = A_Z Z \equiv \begin{bmatrix} 0 & \omega_0 \\ -\omega_0 & 0 \end{bmatrix} Z, \; Z(0) = \begin{bmatrix} \sqrt{2}\,110 \\ 0 \end{bmatrix}, \quad (1)$$

$$y_z \equiv C_Z^T Z = \begin{bmatrix} 1 & 0 \end{bmatrix} Z, \quad (2)$$

where $Z \in \mathbb{R}^2$ is the state of the exosystem and y_z its output. The diagram shown in Figure 1(a), presents the structure of a simple inverter. Figure 1(b) shows the inverter filtered with an $L-C$ filter, to reduce the switching harmonics entering the distribution network.

Before we proceed with the design of the performance, consider an inverter with an $L-C$ filter as shown in Figure 1(b) and a linear resistive load for simplicity in the subsequent analysis. We shall see later that our proposed algorithm is independent of the load and hence can be modeled by any linear or nonlinear functions.

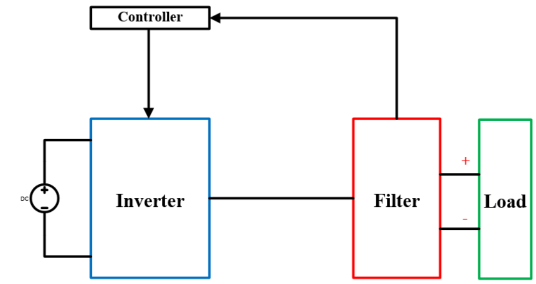

(a) General description of a voltage source inverter.

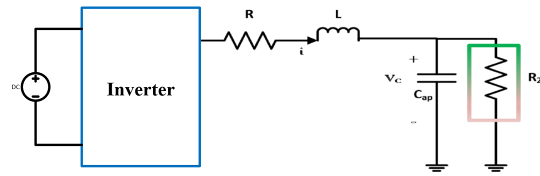

(b) Voltage source inverter filtered by an $L-C$ filter connected to a linear (resistive) load.

Fig. 1. Schematic representation of a power system.

A. State Space Description

The state-space description of the system shown in Figure 1(b) is given by

$$\dot{x} \equiv Ax + Bu = \begin{bmatrix} -\frac{R}{L} & -\frac{1}{L} \\ \frac{1}{C_{\rm ap}} & -\frac{1}{C_{\rm ap}R_2} \end{bmatrix} x + \begin{bmatrix} \frac{1}{L} \\ 0 \end{bmatrix} u, \quad (3)$$

$$y \equiv C^T x = \begin{bmatrix} 0 & 1 \end{bmatrix} x, \quad (4)$$

where the states are $x_1 = i$, $x_2 = V_C$, the output is the voltage across the load and the control input is $u \in \mathbb{R}$ and comes from the inverter.

It is convenient to write the output error $e_{\rm rr} \in \mathbb{R}$ that we would like to drive to zero as,

$$\begin{aligned} e_{\rm rr} &= y - y_z = C^T x - C_Z^T Z \\ &= \begin{bmatrix} 0 & 1 \end{bmatrix} x - \begin{bmatrix} 1 & 0 \end{bmatrix} Z. \end{aligned}$$

B. Performance Design

We need to design a performance index that tracks an exosystem given by (1)-(2) with an unknown frequency by spending the least energy and mapping the input voltage inside the interval $[-V_{\rm dc}, V_{\rm dc}]$. We shall see later that this interval will be finally mapped to $\pm V_{\rm dc}$.

It is desired to minimize an infinite horizon cost functional, but if the optimal tracking control methodology is applied directly for the system (3)-(4) then the performance index should be,

$$J(x(0), e_{\rm rr}(0), u) = \int_0^\infty \left(x^T Q x + R_s(u) + e_{\rm rr}^T Q_r e_{\rm rr} \right) dt \quad (5)$$

where Q, Q_r are user defined nonnegative matrices of appropriate dimensions and to force bounded inputs ($|u| \leqslant V_{\rm dc}$) one has to use $R_s(u) = 2\int_0^u (\theta^{-1}(v))^T dv$, $\forall u$ with $v \in \mathbb{R}$ and $\theta(\cdot)$ a continuous one to one real analytic integrable function of class C_μ, $\mu \geqslant 1$ used to map the interval $[-V_{\rm dc}, V_{\rm dc}]$ on to $\mathbb{R}$. The term $x^T Q x$ constraints the states

Preprint submitted to 2014 American Control Conference.
Received September 27, 2013.

(current, voltage) to encourage a smooth response, whereas the term $e_{\rm rr}^T Q_r e_{\rm rr}$ wants to achieve tracking. Thus the two objectives are conflicting. Hence, the performance index just defined can only regulate and not track.

Hence the next step is to define the tracking problem as a regulator problem following [1]. For that reason we will use an augmented system $\tilde{x} := \begin{bmatrix} x \\ Z \end{bmatrix} \in \mathbb{R}^4$. The dynamics of the augmented state are given by,

$$\begin{aligned} \dot{\tilde{x}} &\equiv \begin{bmatrix} A & 0_{2\times 2} \\ 0_{2\times 2} & A_Z \end{bmatrix} \tilde{x} + \begin{bmatrix} \frac{1}{L} \\ 0_3 \end{bmatrix} u \\ &= \begin{bmatrix} \begin{bmatrix} -\frac{R}{L} & -\frac{1}{L} \\ \frac{1}{C_{\rm ap}} & -\frac{1}{C_{\rm ap} R_2} \end{bmatrix} & 0_{2\times 2} \\ 0_{2\times 2} & \begin{bmatrix} 0 & \omega_0 \\ -\omega_0 & 0 \end{bmatrix} \end{bmatrix} \tilde{x} + \begin{bmatrix} \frac{1}{L} \\ 0_3 \end{bmatrix} u, \quad (6) \end{aligned}$$

with $0_n = \begin{bmatrix} 0 \\ \vdots \\ 0 \end{bmatrix}$ and $O_{n\times n} = \begin{bmatrix} 0 & \cdots & 0 \\ \vdots & \vdots & \vdots \\ 0 & \cdots & 0 \end{bmatrix}$. The following result follows from [1].

Lemma 1: An identical performance index to (5) that tracks the desired exosystem can be defined as,

$$J(\tilde{x}(0), u) = \int_0^\infty \big(R_s(u) + \tilde{x}^T \tilde{Q} \tilde{x}\big) dt, \quad (7)$$

where one has to restrict,

$$\tilde{Q} := \begin{bmatrix} \tilde{Q}_{11} & \tilde{Q}_{12} \\ \tilde{Q}_{21} & \tilde{Q}_{22} \end{bmatrix} \quad (8)$$

with

$$\begin{aligned} C_r &= [I - C(C^T C)^{-1} C^T], \\ \tilde{Q}_{11} &:= C_r^T Q C_r + C Q_r C^T, \\ \tilde{Q}_{12} &:= -(C_r^T Q C_r + C Q_r C^T) C (C^T C)^{-1} C_Z^T, \\ \tilde{Q}_{21} &:= -C_Z (C^T C)^{-1} C^T (C_r^T Q C_r + C Q_r C^T), \\ \tilde{Q}_{22} &:= C_Z (C^T C)^{-1} C^T (C_r^T Q C_r + C Q_r C^T) C \\ &\quad (C^T C)^{-1} C_Z^T. \end{aligned}$$

Proof. For the proof the reader is directed to [1]. ■

Remark 1: Note that a choice for $R_s(u)$ could be $R_s(u) := 2\int_0^u (V_{\rm dc} \tanh^{-1}(\frac{v}{V_{\rm dc}}))^T dv$. □

The ultimate goal is to find the optimal cost function V^* defined by,

$$V^*(\tilde{x}(t)) := \min_u \int_t^\infty \big(R_s(u)) + \tilde{x}^T \tilde{Q} \tilde{x}\big) d\tau, \forall t \geqslant 0, \quad (9)$$

subject to the constraint (6) and given bounded inputs inside the interval $[-V_{\rm dc}, V_{\rm dc}]$.

III. Partial Information Optimal Tracking Control Problem

A. Hamiltonian and Integral Reinforcement Learning

One can define the Hamiltonian associated with (7) and (9) (with V^* the optimal cost function) as,

$$\begin{aligned} H(\tilde{x}, u, \frac{\partial V^*}{\partial \tilde{x}}) &= \big(R_s(u) + \tilde{x}^T \tilde{Q} \tilde{x}\big) \\ &+ \frac{\partial V^*}{\partial \tilde{x}}^T \big(\begin{bmatrix} A & 0_{2\times 2} \\ 0_{2\times 2} & A_Z \end{bmatrix} \tilde{x} + \begin{bmatrix} \frac{1}{L} \\ 0_3 \end{bmatrix} u\big), \ \forall \tilde{x}, u. \quad (10) \end{aligned}$$

We want to find the control input $u(t)$ such that (7) is minimized. Hence we will employ the stationarity condition in the Hamiltonian (10) and we will have

$$\frac{\partial H(\tilde{x}, u, \frac{\partial V^*}{\partial \tilde{x}})}{\partial u} = 0 \Rightarrow u^* = -\theta\{\frac{1}{2} \begin{bmatrix} \frac{1}{L} \\ 0_3 \end{bmatrix}^T \frac{\partial V^*}{\partial \tilde{x}}\}. \quad (11)$$

Remark 2: Note that the control input does not depend on A, A_Z, C, C_Z. □

The optimal cost and the associated constrained optimal control satisfy the following Hamilton-Jacobi-Bellman (HJB) equation,

$$\begin{aligned} H^*(\tilde{x}, u^*, \frac{\partial V^*}{\partial \tilde{x}}) &\equiv \big(R_s(u^*) + \tilde{x}^T \tilde{Q} \tilde{x}\big) \\ &+ \frac{\partial V^*}{\partial \tilde{x}}^T \big(\begin{bmatrix} A & 0_{2\times 2} \\ 0_{2\times 2} & A_Z \end{bmatrix} \tilde{x} + \begin{bmatrix} \frac{1}{L} \\ 0_3 \end{bmatrix} u^*\big) = 0, \ \forall \tilde{x}. \quad (12) \end{aligned}$$

Since the dynamics are required in (12), one needs to find a formulation that allows uncertainties in the dynamics. For that reason we can use an integral reinforcement learning formulation [25] to avoid knowledge of the dynamics for both the system and the exosystem. It has proven in [25] that (10) and the following formulation are equivalent,

$$V(\tilde{x}(t-T)) = \int_{t-T}^t \big(R_s(u) + \tilde{x}^T \tilde{Q} \tilde{x}\big) d\tau + V(\tilde{x}(t)), \ t \geqslant 0 \quad (13)$$

where $T \in \mathbb{R}^+$ is a small time interval that defines how fast we take measurements.

Remark 3: Equation (13) means that we collect information for the state and the control input in the interval $[t-T, t]$ which is tied to learning. This means that in order to collect a large amount of information one needs to pick T sufficiently small however as we will see in the subsequent analysis the convergence will be independent of T. □

The next Theorem proves the existence of the optimal control solution.

Theorem 1: Suppose there exists a positive definite function $V \in C^1$ that satisfies the HJB (12) with $V(0) = 0$. The closed-loop system with,

$$u = -\theta\{\frac{1}{2} \begin{bmatrix} \frac{1}{L} \\ 0_3 \end{bmatrix}^T \frac{\partial V}{\partial \tilde{x}}\} \quad (14)$$

is asymptotically stable. Moreover the control policy (14) is optimal.

Proof. If V satisfies (12) then it also satisfies (10). The orbital derivative along solution (6) and (11) is,

$$\begin{aligned} \dot{V} = \frac{\partial V}{\partial \tilde{x}} \dot{\tilde{x}} &= \frac{\partial V}{\partial \tilde{x}}^T \big(\begin{bmatrix} A & 0_{2\times 2} \\ 0_{2\times 2} & A_Z \end{bmatrix} \tilde{x} + \begin{bmatrix} \frac{1}{L} \\ 0_3 \end{bmatrix} u\big) \\ &= -R_s(u) - \tilde{x}^T \tilde{Q} \tilde{x} \leqslant -\underline{\lambda}(Q) \|\tilde{x}\| \leqslant 0 \end{aligned}$$

where we used (12) with u given by (14). Hence the equilibrium point of (6) is asymptotically stable.

Since the function V is smooth, zero at zero and converge to zero as $t \to \infty$ we can write (7) as,

$$\begin{aligned} J(\tilde{x}(0); u) &= \int_0^\infty \big(R_s(u) + \tilde{x} \tilde{Q} \tilde{x}\big) dt + V^*(\tilde{x}(0)) + \int_0^\infty \dot{V}^* dt \\ &= \int_0^\infty \big(R_s(u) + \tilde{x} \tilde{Q} \tilde{x}\big) dt + V^*(\tilde{x}(0)) \\ &\quad + \int_0^\infty \frac{\partial V^*}{\partial \tilde{x}}^T \big(\begin{bmatrix} A & 0_{2\times 2} \\ 0_{2\times 2} & A_Z \end{bmatrix} \tilde{x} + \begin{bmatrix} \frac{1}{L} \\ 0_3 \end{bmatrix} u\big) dt. \end{aligned}$$

Note that V^* satisfies the HJB (12) and u^* is the optimal policy for the controller given by (11). By subtracting zero we have,

$$J(\tilde{x}(0);u) = \int_0^\infty \Bigg(\big(2(\int_0^u (\theta^{-1}(v))^T dv - \int_0^{u^*} (\theta^{-1}(v))^T dv) \big) + \frac{\partial V^*}{\partial \tilde{x}}^T \begin{bmatrix} \frac{1}{L} \\ 0_3 \end{bmatrix} (u-u^*) \Bigg) dt + V^*(\tilde{x}(0)). \quad (15)$$

By noting that, $\frac{\partial V^*}{\partial \tilde{x}}^T \begin{bmatrix} \frac{1}{L} \\ 0_3 \end{bmatrix} = -2\theta^{-T}(u^*)$ in (15) we can write,

$$J(\tilde{x}(0);u) = \int_0^\infty \Bigg(\big(2(\int_0^u (\theta^{-1}(v))^T dv - \int_0^{u^*} (\theta^{-1}(v))^T dv) \big) - \theta^{-T}(u^*)(u-u^*) \Bigg) dt + V^*(\tilde{x}(0)).$$

We can complete the squares and hence we have,

$$J(\tilde{x}(0);u) = \int_0^\infty \Bigg(2\int_0^{(u-u^*)} (\theta^{-1}(v))^T dv \Bigg) dt + V^*(\tilde{x}(0)).$$

Now by setting $u = u^*$ the following result follows,

$$J^*(\tilde{x}(0);u^*) \equiv V^*(\tilde{x}(0)) \leqslant J(\tilde{x}(0),u).$$

■

B. Actor/Critic Solution

The first step to solve the HJB equation (12) is to approximate the value function $V^*(\tilde{x})$ from (9). The value function can be represented using a critic neural network with N neurons as,

$$V^* = {W^*}^T \phi(\tilde{x}) + \epsilon, \ \forall \tilde{x} \quad (16)$$

where $W^* \in \mathbb{R}^N$ are the ideal weights bounded as $\|W^*\| \leqslant W_{\max}$ and $\phi(\tilde{x})$ is a bounded continuously differentiable basis function ($\|\phi\| \leqslant \phi_{\max}$ and $\left\|\frac{\partial \phi}{\partial \tilde{x}}\right\| \leqslant \phi_{\mathrm{dmax}}$) and ϵ is the residual error such that $\sup_{\tilde{x}} \|\epsilon\| \leqslant \epsilon_{\max}$ and $\sup_{\tilde{x}} \left\|\frac{\partial \epsilon}{\partial \tilde{x}}\right\| \leqslant \epsilon_{\mathrm{dmax}}$. The basis sets are selected such as $N \to \infty$ the functions ϕ provide a complete independent basis for V^*.

By substituting (16) into (11) one has,

$$u^* = -\theta\{\frac{1}{2} \begin{bmatrix} \frac{1}{L} \\ 0_3 \end{bmatrix}^T (\frac{\partial \phi}{\partial \tilde{x}}^T W^* + \frac{\partial \epsilon}{\partial \tilde{x}}^T)\}. \quad (17)$$

The optimal tracking control policy (17) can be approximated by an actor neural network as follows,

$$u^* = {W_u^*}^T \phi_u(\tilde{x}) + \epsilon_u(\tilde{x}), \forall \tilde{x},$$

where $W_u^* \in \mathbb{R}^{N_2}$ are the optimal weights, $\phi_u(\tilde{x})$ are the NN activation functions defined similarly to the critic NN, N_2 is the number of neurons in the hidden layer and ϵ_u is the actor approximation error. Note that the NN activation functions must define a complete independent basis set such that u^* is uniformly approximated.

Assumption 1: The approximation error ϵ_u is bounded by a known constant $\epsilon_{\mathrm{umax}} \in \mathbb{R}^+$. Furthermore the activation functions ϕ_u are upper bounded by $\phi_{\mathrm{umax}} \in \mathbb{R}^+$. □

By using (17) into (13) one has,

$${W^*}^T \phi(\tilde{x}(t)) - {W^*}^T \phi(\tilde{x}(t-T)) + \int_{t-T}^t \big(R_s(u^*) + \tilde{x}^T \tilde{Q} \tilde{x}\big) d\tau = \epsilon_\pi.$$

where ϵ_π is bounded on $\mathbb{R}^n$ and $T > 0$.

We define the integral reinforcement as

$$\pi(t) = \int_{t-T}^t \big(R_s(u^*) + \tilde{x}^T \tilde{Q} \tilde{x}\big) d\tau, t \geqslant 0$$

and now (13) can be written as,

$${W^*}^T \Delta\phi(\tilde{x}(t)) + \pi(t) = \epsilon_\pi,$$

where $\Delta\phi(\tilde{x}(t)) := \phi(\tilde{x}(t)) - \phi(\tilde{x}(t-T))$ and ϵ_π is a function of the residual error ϵ.

The value function and optimal policy using current estimates $\hat{W}$ and $\hat{W}_u$ respectively of the ideal weights W^* and W_u^* are given by the following critic and actor neural networks,

$$\hat{V} = \hat{W}^T \phi(\tilde{x}(t)), \ \forall \tilde{x} \quad (18)$$

$$\hat{u} = \hat{W}_u^T \phi_u(\tilde{x}(t)), \ \forall \tilde{x}. \quad (19)$$

Now after using the approximations for $\hat{V}$ given by (18) and for $\hat{u}$ given by (19), we can write the measurable form of (13) as the error $e \in \mathbb{R}$ given by,

$$e := \hat{W}^T \Delta\phi(\tilde{x}(t)) - \hat{\pi}, \forall \tilde{x}$$

where $\hat{\pi} := \int_{t-T}^t \big(R(\hat{u}) + \tilde{x}^T \tilde{Q} \tilde{x}\big) d\tau$. In order to drive the error e to zero, one has to pick the neural networks weights appropriately using adaptive control techniques [10].

For that reason it is desired to select the critic weights $\hat{W}$ to minimize a squared error of the form $E = \frac{1}{2}e^2$. The gradient descent algorithm gives,

$$\dot{\hat{W}} = -\alpha \frac{\Delta\phi(\tilde{x}(t))}{(\Delta\phi(\tilde{x}(t))^T \Delta\phi(\tilde{x}(t)) + 1)^2} (\Delta\phi(\tilde{x}(t))^T \hat{W} + \hat{\pi}), \quad (20)$$

where $\alpha \in \mathbb{R}^+$ determines the speed of convergence. Define the critic and actor estimation errors as,

$$\tilde{W} := W^* - \hat{W}; \ \tilde{W}_u := W_u^* - \hat{W}_u.$$

The critic error dynamics can be written as,

$$\dot{\tilde{W}} = -\alpha \frac{\Delta\phi(\tilde{x}(t)) \Delta\phi(\tilde{x}(t))^T}{(\Delta\phi(\tilde{x}(t))^T \Delta\phi(\tilde{x}(t)) + 1)^2} \tilde{W} + \alpha \frac{\Delta\phi(\tilde{x}(t))}{(\Delta\phi(\tilde{x}(t))^T \Delta\phi(\tilde{x}(t)) + 1)^2} \epsilon_\pi \equiv -N_{\mathrm{om}} + p_{\mathrm{er}}, \quad (21)$$

where N_{om} is the nominal system and p_{er} is the perturbation due to the error ϵ_π.

Theorem 2: Let the tuning of the critic neural network be given by (20). Then the nominal system N_{om} from (21) is exponentially stable with its trajectories satisfying $\left\|\tilde{W}(t)\right\| \leqslant \left\|\tilde{W}(t_0)\right\| \kappa_1 e^{-\kappa_2(t-t_0)}$, for $t > t_0 \geqslant 0$, for some $k_1, k_2 \in \mathbb{R}^+$ provided that the signal $M := \frac{\Delta\phi(\tilde{x}(t))}{(\Delta\phi(\tilde{x}(t))^T \Delta\phi(\tilde{x}(t)) + 1)}$ is persistently exciting over the interval $[t, t+T_{\mathrm{PE}}]$ with $\int_t^{t+T_{\mathrm{PE}}} MM^T d\tau \geqslant \beta I$.

Proof. See [25] for the proof. ■

Now define the actor error $e_u \in \mathbb{R}$ as,

$$e_u := \hat{W}_u^T \phi_u + \theta\{\frac{1}{2} \begin{bmatrix} \frac{1}{L} \\ 0_3 \end{bmatrix}^T (\frac{\partial \phi}{\partial \tilde{x}}^T \hat{W})\}.$$

Preprint submitted to 2014 American Control Conference.
Received September 27, 2013.

The objective is to select $\hat{W}_u$ such that the following criterion is minimized,

$$E_u = \frac{1}{2} e_u^T e_u. \tag{22}$$

The tuning for the actor weights $\hat{W}_u$ can be found by applying gradient descent to (22),

$$\dot{\hat{W}}_u = -\alpha_u \phi_u \left(\hat{W}_u^T \phi_u + \theta\{\frac{1}{2} \begin{bmatrix} \frac{1}{L} \\ 0_3 \end{bmatrix}^T (\frac{\partial \phi}{\partial \tilde{x}}^T \hat{W})\} \right)^T, \tag{23}$$

where $\alpha_u \in \mathbb{R}^+$ determines the speed of convergence.

Using a similar approach with the critic error dynamics we can write the actor error dynamics as,

$$\begin{aligned} \dot{\tilde{W}}_u &= -\alpha_u \phi_u \phi_u^T \tilde{W}_u - \alpha_u \phi_u \epsilon_u \\ &- \alpha_u \phi_u \theta\{\frac{1}{2} \tilde{W}^T \frac{\partial \phi}{\partial \tilde{x}} \begin{bmatrix} \frac{1}{L} \\ 0_3 \end{bmatrix}\} - \alpha_u \phi_u \theta\{\frac{1}{2} \frac{\partial \epsilon}{\partial \tilde{x}} \begin{bmatrix} \frac{1}{L} \\ 0_3 \end{bmatrix}\}. \end{aligned} \tag{24}$$

Remark 4: Note that in order to implement the algorithm one needs to measure the current and the voltage of the $L-C$ filter and needs to know only the L, since only L appears in the neural network tuning laws. □

Note that the control input (19) has to provide DC voltage $\pm V_{\rm dc}$ and not inside $[-V_{\rm dc}, V_{\rm dc}]$. For that reason one should pass the control input from a hard limiter that limits its output to $\pm V_{\rm dc}$, i.e.

$$\hat{u}_{\rm dc} = V_{\rm dc}\ \theta_{\rm hlim}(\hat{u});\ \theta_{\rm hlim}(\hat{u}) = \begin{cases} -1, & \hat{u} < 0 \\ 1, & \hat{u} >= 0. \end{cases}$$

A block diagram showing the proposed control architecture for the voltage source inverter is shown in Figure 2.

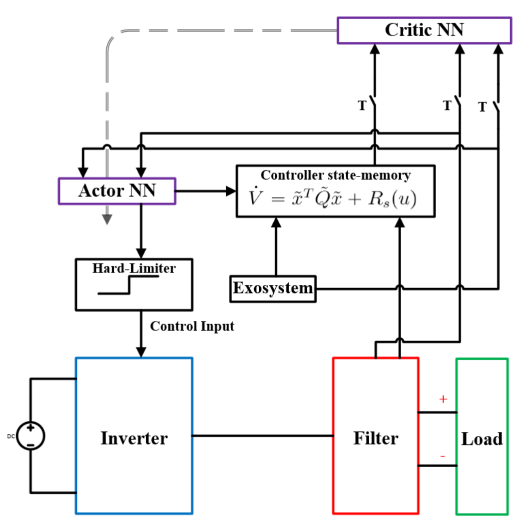

Fig. 2. Visualization of the proposed control architecture for a voltage source inverter where T represents how fast we are taking measurements of the the exosystem and the voltage and the current of the filter by opening and closing three switches. Note that the dashed line shows that the actor is being tuned based on the performance which is computed by the critic NN.

C. Convergence and Stability Analysis

Fact 1: The following normalized signal satisfies,

$$\left\| \frac{\Delta\phi(\tilde{x}(t))}{(\Delta\phi(\tilde{x}(t))^T \Delta\phi(\tilde{x}(t)) + 1)} \right\| \leqslant \Delta_{\max} := \frac{1}{2}.$$

Moreover, the following bounds are used to simplify the results from the following Theorem and are consequences of previous Assumptions ,

$$\|\theta(\cdot)\| \leqslant V_{\rm dc};\ \|\epsilon_\pi\| \leqslant \epsilon_{\pi\max}.$$

□

To deal with the presence of the neural network approximation errors and known bounds [19], and obtain an asymptotically stable closed-loop system one needs to add a robustifying term to the closed loop system of the form,

$$\eta(t) = -\begin{bmatrix} \frac{1}{L} \\ 0_3 \end{bmatrix} \frac{\|\tilde{x}\|^2}{K_1 + \|\tilde{x}\|^2} K_2, \tag{25}$$

where $K_1, K_2 \in \mathbb{R}^+$ satisfy,

$$\begin{aligned} K_2 > L & \frac{K_1 + \|\tilde{x}\|^2}{\|\tilde{x}\|^2 (W_{\max}\phi_{\rm dmax} + \epsilon_{\rm dmax})} \\ & \Big\{ (\frac{W_{\max}\phi_{\rm dmax} + \epsilon_{\rm dmax}}{L} \phi_{\rm umax})^2 + \epsilon_{\rm umax}^2 \\ & + (\frac{W_{\max}\phi_{\rm dmax} + \epsilon_{\rm dmax}}{L})^2 + \left(2\Delta_{\max}^2 \epsilon_{\pi\max}\right)^2 \\ & + \left(\phi_{\rm umax}\epsilon_{\rm umax} + 2\phi_{\rm umax} V_{\rm dc}\right)^2 \Big\}. \end{aligned} \tag{26}$$

The system dynamics (6) by using the robustifying term (25) can be written as,

$$\begin{aligned} \dot{\tilde{x}} \equiv & \begin{bmatrix} A & 0_{2\times2} \\ 0_{2\times2} & A_Z \end{bmatrix} \tilde{x} \\ & + \begin{bmatrix} \frac{1}{L} \\ 0_3 \end{bmatrix} \left((W_u^* - \tilde{W}_u)^T \phi_u(\tilde{x}) - K_2 \frac{\|\tilde{x}\|^2}{K_1 + \|\tilde{x}\|^2} \right). \end{aligned} \tag{27}$$

The following theorem is the main result and proves asymptotic stability of the overall system and convergence to the optimal solution.

Theorem 3: Consider the dynamics (6) with the control input given by (19) and the $\tilde{Q}$ picked according to (8). The tuning laws for the critic and actor neural network are given by (20) and (23) respectively and the learning information collecting interval T is picked sufficiently small. Then the equilibrium point of $\left(\tilde{x}(t), \tilde{W}(t), \tilde{W}_u(t)\right)$ is asymptotically stable for all $\left(\tilde{x}(0), \tilde{W}(0), \tilde{W}_u(0)\right)$ and the output of the system at the load provides the appropriate voltage frequency and magnitude by following the exosystem, provided that the following inequalities are satisfied,

$$\phi_{\rm umax} \geqslant 1;\ \alpha \geqslant \frac{1}{2}. \tag{28}$$

□

Remark 5: The persistence of excitation (PE) condition is standard in adaptive control techniques [10] and very important for neural network convergence. The PE ensures that the time varying signal $\frac{\Delta\phi(\tilde{x}(t))}{(\Delta\phi(\tilde{x}(t))^T \Delta\phi(\tilde{x}(t))+1)}$ rotates sufficiently in space. □

D. Proof of Theorem 3

Proof. Consider the following Lyapunov equation $\mathcal{V}:\mathbb{R}^4\times\mathbb{R}^N\times\mathbb{R}^{N_2}\to\mathbb{R}$ for all $t\geqslant 0$ defined as,

$$\begin{aligned}\mathcal{V}&=V^*+V_c+V_u,\\ &\equiv V^*+V_c+\frac{1}{2\alpha_u}\{\tilde{W}_u^T\tilde{W}_u\}\end{aligned}\tag{29}$$

where V^* is the optimal value function and $V_c:=\left\|\tilde{W}\right\|^2$ is a Lyapunov function for the critic error dynamics given by (21).

By taking the time derivative of (29) (first term with respect to (27), second term with respect to the perturbed critic estimation error dynamics (21) as shown in Theorem 2, and substitute the actor error dynamics from (24)) and grouping the terms together, one has,

$$\begin{aligned}\dot{\mathcal{V}}=&\frac{\partial V^*}{\partial\tilde{x}}^T\Big(\begin{bmatrix}A & 0_{2\times2}\\ 0_{2\times2} & A_Z\end{bmatrix}\tilde{x}\\ &+\begin{bmatrix}\frac{1}{L}\\ 0_3\end{bmatrix}\big((W_u^*-\tilde{W}_u)^T\phi_u(\tilde{x})-K_2\frac{\|\tilde{x}\|^2}{K_1+\|\tilde{x}\|^2}\big)\Big)\\ &-\frac{\partial V_c}{\partial\tilde{W}}^T\Big(\frac{\Delta\phi(\tilde{x}(t))\Delta\phi(\tilde{x}(t))^T}{(\Delta\phi(\tilde{x}(t))^T\Delta\phi(\tilde{x}(t))+1)^2}\Big)\tilde{W}\\ &+\frac{\partial V_c}{\partial\tilde{W}}^T\Big(\frac{\Delta\phi(\tilde{x}(t))}{(\Delta\phi(\tilde{x}(t))^T\Delta\phi(\tilde{x}(t))+1)^2}\epsilon_\pi\Big)\\ &+\{\tilde{W}_u^T\big(-\phi_u\phi_u^T\tilde{W}_u-\phi_u\epsilon_u-\phi_u\theta\{\frac{1}{2}\begin{bmatrix}\frac{1}{L}\\ 0_3\end{bmatrix}^T\big(\frac{\partial\phi}{\partial\tilde{x}}^T\tilde{W}\big)\}\\ &-\phi_u\theta\{\frac{1}{2}\begin{bmatrix}\frac{1}{L}\\ 0_3\end{bmatrix}\frac{\partial\epsilon}{\partial\tilde{x}}^T\}\big)\},t\geqslant 0.\end{aligned}\tag{30}$$

Now for simplicity we will take the following two terms of (30) separately as,

$$\begin{aligned}T_1:=&\frac{\partial V^*}{\partial\tilde{x}}^T\Big(\begin{bmatrix}A & 0_{2\times2}\\ 0_{2\times2} & A_Z\end{bmatrix}\tilde{x}\\ &+\begin{bmatrix}\frac{1}{L}\\ 0_3\end{bmatrix}\big((W_u^*-\tilde{W}_u)^T\phi_u(\tilde{x})-K_2\frac{\|\tilde{x}\|^2}{K_1+\|\tilde{x}\|^2}\big)\Big)\end{aligned}\tag{31}$$

and

$$\begin{aligned}T_2:=&-\frac{\partial V_c}{\partial\tilde{W}}^T\Big(\frac{\Delta\phi(\tilde{x}(t))\Delta\phi(\tilde{x}(t))^T}{(\Delta\phi(\tilde{x}(t))^T\Delta\phi(\tilde{x}(t))+1)^2}\Big)\tilde{W}\\ &+\frac{\partial V_c}{\partial\tilde{W}}^T\Big(\frac{\Delta\phi(\tilde{x}(t))}{(\Delta\phi(\tilde{x}(t))^T\Delta\phi(\tilde{x}(t))+1)^2}\epsilon_\pi\Big)\\ &+\tilde{W}_u^T\big(-\phi_u\phi_u^T\tilde{W}_u-\phi_u\epsilon_u-\phi_u\theta\{\frac{1}{2}\begin{bmatrix}\frac{1}{L}\\ 0_3\end{bmatrix}^T\big(\frac{\partial\phi}{\partial\tilde{x}}^T\tilde{W}\big)\}\\ &-\phi_u\theta\{\frac{1}{2}\begin{bmatrix}\frac{1}{L}\\ 0_3\end{bmatrix}\frac{\partial\epsilon}{\partial\tilde{x}}^T\}\big).\end{aligned}\tag{32}$$

Now using (12) in (31) one has,

$$\begin{aligned}T_1=&-R_s(u^*)-\tilde{x}^T\tilde{Q}\tilde{x}-\frac{\partial V^*}{\partial\tilde{x}}^T\begin{bmatrix}\frac{1}{L}\\ 0_3\end{bmatrix}\tilde{W}_u^T\phi_u(\tilde{x})\\ &-\frac{\partial V^*}{\partial\tilde{x}}^T\begin{bmatrix}\frac{1}{L}\\ 0_3\end{bmatrix}\epsilon_u-\frac{\partial V^*}{\partial\tilde{x}}^T\begin{bmatrix}\frac{1}{L}\\ 0_3\end{bmatrix}K_2\frac{\|\tilde{x}\|^2}{K_1+\|\tilde{x}\|^2}\end{aligned}$$

which can be upper bounded as,

$$\begin{aligned}T_1\leqslant&-R_s(u^*)-\tilde{x}^T\tilde{Q}\tilde{x}-\frac{(W_{\max}\phi_{\text{dmax}}+\epsilon_{\text{dmax}})}{L}\\ &(\phi_{\text{umax}}\left\|\tilde{W}_u\right\|+\epsilon_{\text{umax}}+K_2\frac{\|\tilde{x}\|^2}{K_1+\|\tilde{x}\|^2}).\end{aligned}\tag{33}$$

By using Young's inequality for products one can further upper bound (33) as,

$$\begin{aligned}T_1\leqslant&-R_s(u^*)-\underline{\lambda}(\tilde{Q})\|\tilde{x}\|^2\\ &+\frac{1}{2}\big(\frac{W_{\max}\phi_{\text{dmax}}+\epsilon_{\text{dmax}}}{L}\phi_{\text{umax}}\big)^2\\ &+\frac{1}{2}\left\|\tilde{W}_u\right\|^2+\frac{1}{2}\epsilon_{\text{umax}}^2+\frac{1}{2}\big(\frac{W_{\max}\phi_{\text{dmax}}+\epsilon_{\text{dmax}}}{L}\big)^2\\ &-\frac{(W_{\max}\phi_{\text{dmax}}+\epsilon_{\text{dmax}})}{L}K_2\frac{\|\tilde{x}\|^2}{K_1+\|\tilde{x}\|^2}.\end{aligned}$$

Now we can upper bound (32) by using the results from Theorem 2 as

$$\begin{aligned}T_2\leqslant&-\alpha\left\|\tilde{W}\right\|^2-\phi_{\text{umax}}^2\left\|\tilde{W}_u\right\|^2+2\Delta_{\max}^2\epsilon_{\pi\max}\left\|\tilde{W}\right\|\\ &-\big(\phi_{\text{umax}}\epsilon_{\text{umax}}+2\phi_{\text{umax}}V_{\text{dc}}\big)\left\|\tilde{W}_u\right\|.\end{aligned}\tag{34}$$

By using Young's inequality for products one can further upper bound (34) as,

$$\begin{aligned}T_2\leqslant&-\alpha\left\|\tilde{W}\right\|^2-\phi_{\text{umax}}^2\left\|\tilde{W}_u\right\|^2\\ &+\frac{1}{2}\big(2\Delta_{\max}^2\epsilon_{\pi\max}\big)^2+\frac{1}{2}\left\|\tilde{W}\right\|^2\\ &+\frac{1}{2}\Big(\big(\phi_{\text{umax}}\epsilon_{\text{umax}}+2\phi_{\text{umax}}V_{\text{dc}}\big)\Big)^2+\frac{1}{2}\left\|\tilde{W}_u\right\|^2.\end{aligned}$$

Finally (30) can be written as, $\dot{\mathcal{V}}\leqslant T_1+T_2$ and after taking into consideration the bound of K_2 given by (26) one has,

$$\begin{aligned}\dot{\mathcal{V}}\leqslant&-R_s(u^*)-\underline{\lambda}(\tilde{Q})\|\tilde{x}\|^2\\ &-(\phi_{\text{umax}}^2-1)\left\|\tilde{W}_u\right\|^2-(\alpha-\frac{1}{2})\left\|\tilde{W}\right\|^2.\end{aligned}$$

By taking into account the inequalities (28) one has $\dot{\mathcal{V}}<0, t\geqslant 0$. From Barbalat's lemma [13] it follows that as $t\to\infty$, then $\|e_{\text{rr}}\|\to 0$, $\left\|\tilde{W}\right\|\to 0$ and $\left\|\tilde{W}_u\right\|\to 0$ and hence the robustifying term goes to zero asymptotically. Finally since the robustifying term goes to zero hence $\|u\|\to u^*$. ■

IV. SIMULATIONS

Consider the DC/AC inverter shown in Figure 1(b) with $L=2mH, C_{\text{ap}}=10\mu F, R=0.1\Omega$. The user defined matrices are defined as $Q=\begin{bmatrix}0.1 & 0\\ 0 & 0.2\end{bmatrix}$ and Q_r identity, $\tilde{Q}$ is found from (8) and the control input is $\pm V_{\text{dc}}$ with $V_{\text{dc}}=5$ after passed from the hard limiter. In the actual implementation of the algorithm the values of the parasitic resistance R, the capacitance C_{ap}, the load (linear/nonlinear) and the frequency of the exosystem ω_0 which in most of the cases in real world are not known exactly, are not needed. The tuning gains are picked as $\alpha=20$ and $\alpha_u=1$.

A. Linear Load

The algorithm from Theorem 3 is applied by considering a simple linear resistive load (in the algorithm proposed this is considered unknown) as described in the previous sections with $R_2=12.5\Omega$. The algorithm needs only 0.0002 secs for learning. In Figures 3(a)-3(b) one can see the desired output voltage versus the actual one. The tracking error is negligible since the output AC voltage has a magnitude of $110\sqrt{2}$ V and a frequency of 60 Hz. One can see in Figure 4(a) that the

Preprint submitted to 2014 American Control Conference.
Received September 27, 2013.

frequency of the control input (pulse-like waveform of ± 5) has the same frequency to that of the desired AC waveform rather than much higher as in most of the inverters. This is an adding improvement in terms of bandwidth. Figure 4(b) shows the evolution of the current at the load which is a pure cosine since we have a resistive load. Figure 5 shows the power dissipated in the purely resistive load which is a series of positive pulses. This is because the resultant power is positive when the voltage and current are both in their positive half cycle.

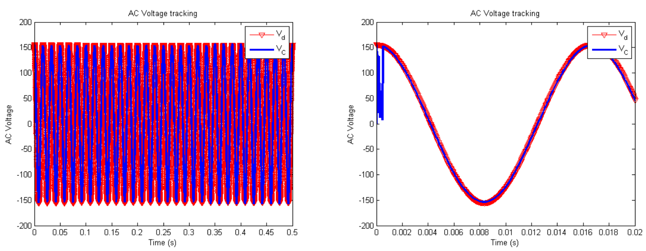

(a) Voltage tracking. (b) Detailed Initial Tracking.

Fig. 3. AC Voltage with a magnitude of $110\sqrt{2}$ Volts and a frequency of 60 Hz is produced at the output.

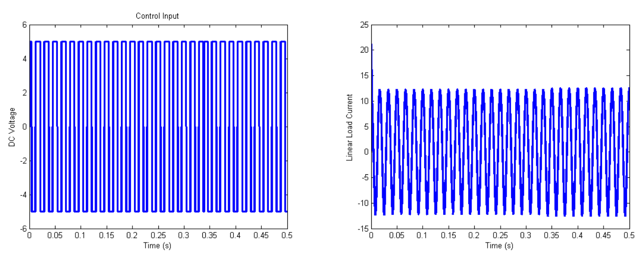

(a) Control input provides ± 5 V. (b) Load current evolution.

Fig. 4. Control input is $\pm V_{\rm dc}$ while the load current is a pure cosine since we have a linear load connected to the $L - C$ filter.

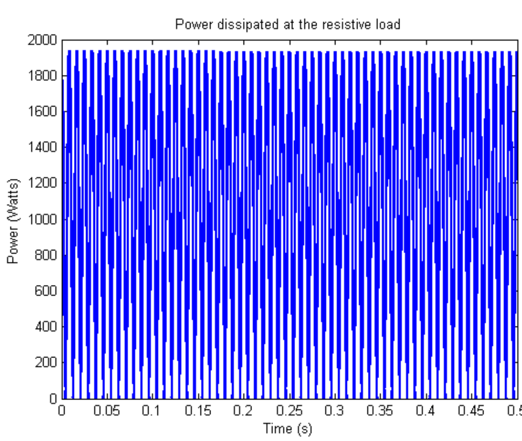

Fig. 5. Power dissipated at the resistive load.

B. Nonlinear Load

A nonlinear load model adopted from a fluorescent lamp model with an unknown equivalent resistance variation [6] is simulated using the proposed algorithm. Figure 6 shows the evolution of the current at the load which is a non-cosinusoidal waveform with different harmonics. The output voltage is similar to Figures 3(a)-3(b) and thus is omitted due to space limitations.

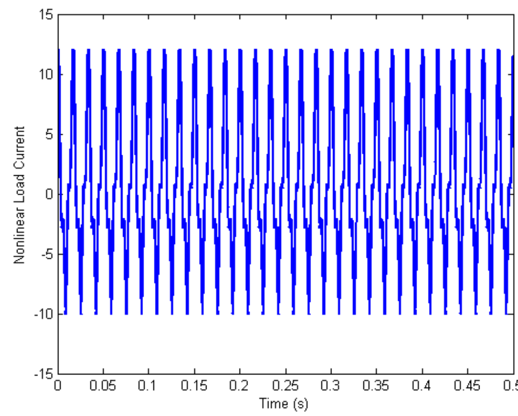

Fig. 6. Evolution of the current at the nonlinear load.

V. Conclusion and Future Work

This paper proposed an intelligent optimal tracking controller that provides the desired magnitude and frequency at the load that works as a DC/AC microinverter that converts low DC voltage to high AC voltage. The controller ensures a good tracking of the output voltage with guaranteed performance. The algorithm builds upon the ideas of ADP and uses only partial information of the system and the exosystem that provides the desired behavior without any phasor domain analysis. Simulation results showed the effectiveness of the proposed approach. Future work will be concentrated on extending the results for synchronizing completely unknown inverters.

References

[1] B. D. O Anderson and J. B. Moore, *Linear Optimal Control*, Englewood Cliffs, Prentice Hall, NJ, 1971
[2] A. R. Bergen, V. Vittal, *Power Systems Analysis*, Pearson/Prentice Hall, 2000
[3] B. Bolsens, K.de Branbandere, J. Van den Keybus, J. Driesen, R. Belmans. "Model-Based Generation of Low Distortion Currents in Grid-Coupled PWMInverters Using an LCL Output Filter," *35th Annual IEEE PESC*, pp. 4616-4622, 2004
[4] E. J. Bueno, F. Espinosa, F. J. Rodriguez, J. Urena, S. Cobreces. "Current Control of Voltage Source Converters connected to the grid through an LCL- filter," *Proc. 25th Annual IEEE Power Electronics Specialists Conference*, pp. 68-73, 2004
[5] S. R. Bull, "Renewable energy today and tomorrow," *Proc. IEEE*, vol. 89, no. 8, pp. 1216-1226, 2001
[6] M. Cervi, A. R. Seidel, F. E. Bisogno and D. Prado, "Fluorescent Lamp Model based on the Equivalent Resistance Variation," *Proc. IEEE Intl. Conf. on Ind. Appl.*, pp. 680-684, 2002
[7] D. Ernst, M. Glavic, and L. Wehenkel, "Power systems stability control: Reinforcement learning framework," *IEEE Trans. Power Syst.*, vol. 19, no. 1, pp. 427435, 2004
[8] R.M. Santos Filho, P. F. Seixas, P.C. Cortizo, L. Torres, A.F. Souza, "Comparison of Three Single-Phase PLL Algorithms for UPS Applications," *IEEE Transactions on Industrial Electronics*, vol.55, no.8, pp. 2923-2932, 2008 vol. 15, pp. 486-505, 1977

Preprint submitted to 2014 American Control Conference.
Received September 27, 2013.

[9] T. G. Habetler, "A space vector-based rectifier regulator for AC/DC/AC converters," *IEEE Transactions on Power Electronics*, vol.8, no.1, pp. 30-36, 1993

[10] P. A. Ioannou, B. Fidan, *Adaptive Control Tutorial*, Advances in design and control, SIAM (PA), 2006

[11] T. Kawabata, T. Miyashita, Y. Yamamoto. "Dead Beat Control of Three Phase PWM Inverter," *IEEE Trans. on Power Electronics*, vol. 5, no. 1, pp. 21-28, 1990

[12] Yu Jiang, Zhong-Ping Jiang, "Robust Adaptive Dynamic Programming With an Application to Power Systems," *IEEE Transactions on Neural Networks and Learning Systems*, vol.24, no.7, pp. 1150-1156, 2013

[13] H. K. Khalil, *Nonlinear Systems*, Prentice Hall, 2002

[14] P. Kundur, N. J. Balu, and M. G. Lauby, *Power System Stability and Control*, New York: McGraw-Hill, 1994

[15] F. L. Lewis, D. Vrabie, K. G. Vamvoudakis, "Reinforcement Learning and Feedback Control: Using Natural Decision Methods to Design Optimal Adaptive Controllers," *IEEE Control Systems*, vol.32, no.6, pp.76-105, 2012

[16] M. Lindgren, J. Svensson. "Control of a Voltage-source Converter Connected to the Grid through an LCL-filter - Application to Active Filtering," *Proc. IEEE PESC*, pp.229-235, 1998

[17] S. Mariethoz, A. G. Beccuti, M. Morari, "Analysis and optimal current control of a voltage source inverter connected to the grid through an LCL filter," *IEEE Power Electronics Specialists Conference*, pp. 2132-2138, 2008

[18] S. Mohagheghi, Y. del Valle, G. K. Venayagamoorthy, and R. G. Harley, "A proportional-integrator type adaptive critic design-based neurocontroller for a static compensator in multimachine power systems," *IEEE Trans. Ind. Electron.*, vol. 54, no. 1, pp. 8696, 2007

[19] M. Polycarpou, J. Farrell, M. Sharma, "On-line approximation control of uncertain nonlinear systems: issues with control input saturation," *Proc. American Control Conference*, pp.543,548 2003

[20] M. Prodanovic, T. C. Green. "Control and Filter Design of Three-Phase Inverters for High Power Quality Grid Connection," *IEEE Trans. on Power Electronics*, vol. 18, no. 1, pp. 373-380, 2003

[21] E. Twining, D. G. Holmes, "Grid Current Regulation of a Three-Phase Voltage Source Inverter With an LCL Input Filter," *IEEE Trans. on Power Electronics*, vol. 18, no. 3, pp. 888-895, 2003

[22] Y. del Valle, G. K. Venayagamoorthy, S. Mohagheghi, J. C. Hernandez, and R. G. Harley, "Particle swarm optimization: Basic concepts, variants and applications in power systems," *IEEE Trans. Evol. Comput.*, vol. 12, no. 2, pp. 171195, 2008

[23] G. K. Venayagamoorthy, D. C. Wunsch, and R. G. Harley, "Applications of Approximate Dynamic Programming in Power Systems Control," in *Handbook of Learning and Approximate Dynamic Programming*, pp. 479-515, 2004

[24] G. K. Venayagamoorthy, "Dynamic, Stochastic, Computational, and Scalable Technologies for Smart Grids," *IEEE Computational Intelligence Magazine*, vol.6, no.3, pp.22-35, 2011

[25] D. Vrabie, K. G. Vamvoudakis, F. L. Lewis, *Optimal Adaptive Control and Differential Games by Reinforcement Learning Principles*, Control Engineering Series, IET Press, 2012

[26] F. Zare and J. A. Firouzjaee, "Hysteresis band current control for a single phase Z-source inverter with symmetrical and asymmetrical Znetwork," *Proc. Power Convers. Conf.*, pp. 143148, 2007

[27] D. N. Zmood, D. G. Holmes, G. H. Bode, "Frequency-Domain Analysis of Three-Phase Linear Current Regulator," *IEEE Trans. on Industry Applications*, Vol. 37, No. 2, pp. 601-610, 2001

Preprint submitted to 2014 American Control Conference.
Received September 27, 2013.